Electromagnetism based atmospheric ice sensing technique - A conceptual review

Umair N. Mughal*, Muhammad S. Virk and M. Y. Mustafa
High North Technology Center
Department of Technology, Narvik University College, Narvik, Norway

ABSTRACT

Electromagnetic and vibrational properties of ice can be used to measure certain parameters such as ice thickness, type and icing rate. In this paper we present a review of the dielectric based measurement techniques for matter and the dielectric/spectroscopic properties of ice. Atmospheric Ice is a complex material with a variable dielectric constant, but precise calculation of this constant may form the basis for measurement of its other properties such as thickness and strength using some electromagnetic methods. Using time domain or frequency domain spectroscopic techniques, by measuring both the reflection and transmission characteristics of atmospheric ice in a particular frequency range, the desired parameters can be determined.

Keywords: Atmospheric Ice, Sensor, Polar Molecule, Quantum Excitation, Spectroscopy, Dielectric

1. INTRODUCTION

1.1. ATMOSPHERIC ICING

Atmospheric icing is the term used to describe the accretion of ice on structures or objects under certain conditions. This accretion can take place either due to freezing precipitation or freezing fog. It is primarily freezing fog that causes this accumulation which occurs mainly on mountaintops [16]. It depends mainly on the shape of the object, wind speed, temperature, liquid water content (amount of liquid water in a given volume of air) and droplet size distribution (conventionally known as the median volume diameter).

The major *effects of atmospheric icing* on structure are the static ice loads, wind action on iced structure and dynamic effects.

Generally an icing event is defined as periods of time where the temperature is below 0°C and the relative humidity is above 95%. Ice accretion can be defined as, *any process of ice build up and snow accretion on the surface of objects exposed to the atmosphere'* [12]. Atmospheric icing is traditionally classified according to two different processes [12] and are shown in Fig. 1(a),

(a) Precipitation icing (including freezing precipation and wet snow),
(b) In-cloud icing (also called rime/glaze, including fog),

Fig. l(b) shows the type of accreted ice as a function of wind speed and temperature. In this figure, the curve shifts to the left with the increasing liquid water content and with decreasing object size. A classification of atmospheric ice is shown in Table 1.

*Corresponding author. E-mail: umair.mughal@gmail.com

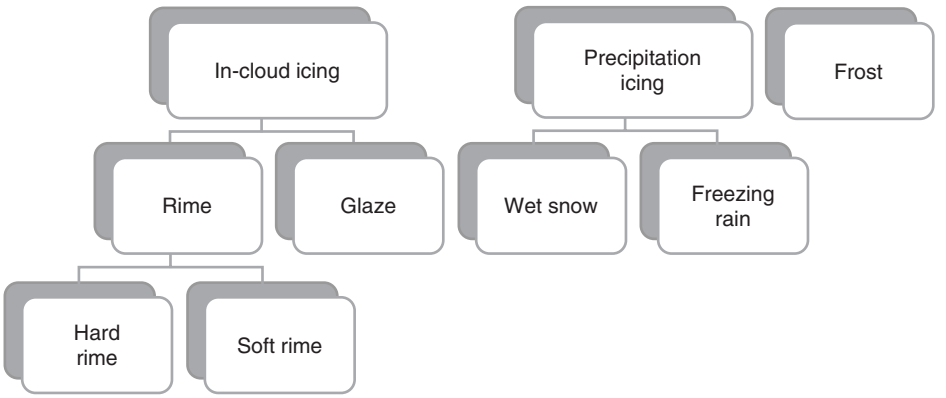

(a) Ice types

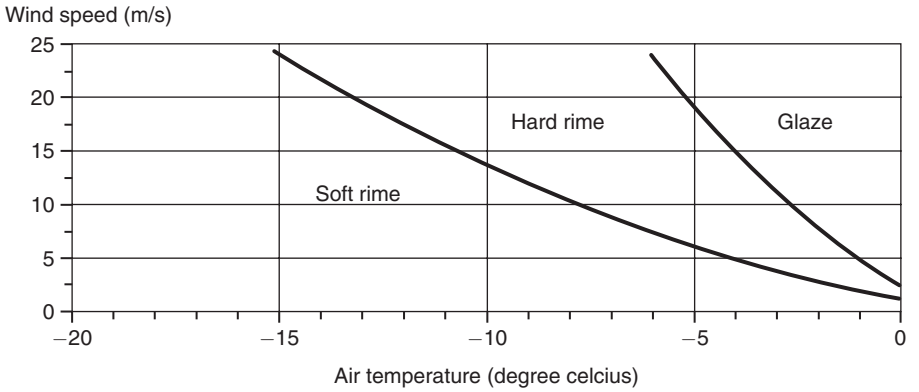

(b) Ice as a function of wind speed and air temperature

Figure 1 Ice types and their dependence [12].

Table 1 Typical properties of accreted atmospheric ice [11].

		Adhesion &	General appearance	
Type of ice	**Density (kg/m^3)**	**Cohesion**	**Colour**	**Shape**
Glaze	900	strong	transparent	evenly distributed/icicles
Wet snow	300–600	weak, strong	white	evenly distributed/eccentric
Hard rime	600–900	strong	opaque	eccentric, pointing windward
Soft rime	200–600	low to medium	white	eccentric pointing windward

1.2. ATMOSPHERIC ICING SENSORS

The main purpose of an ice detector is to detect and indicate the rate of an icing event. Depending on the type of accreted ice, glaze or rime, deicing power requirements will be different, therefore it is important for the ice detection sensor to distinguish between rime and glaze ice. Ice detection methods can be categorized as *direct methods* and *indirect methods.*

The *indirect methods* of ice detection involves measuring weather conditions such as humidity, temperature, pressure, etc. that creates proper circumstances for an icing event to

occur. For example, reduction in the power generated by the wind turbine, reduction in the speed of anemenometers or measuring the variables that cause icing or variables that correlate with the occurrence of icing, such as cloud height and visibility [11]. Empirical or deterministic models are then used to determine when icing is expected to occur [15]. The reduction in the speed of anemenometers of Craig and Craig [7] and the noise generation frequency method of Seifert [23] are typical examples of indirect methods.

The *direct methods* of ice detection are based on the principle of detecting property changes caused by ice accretion. Examples of such properties include the mass and dielectric constant. The inductance change probe of Lee and Seegmiller [22], the impedance change probe of Wallace et. al. [25] and the microwave ice detector of Magenheim [21] are examples of direct methods.

There are presently few available instruments in the market. However there are some prototype instruments which seem very promising and may lead to interesting products after thorough testing and verifications. These instruments are based on different working principles. In [15] it is mentioned that there are about 24 direct methods and 5 indirect methods of ice measurements.

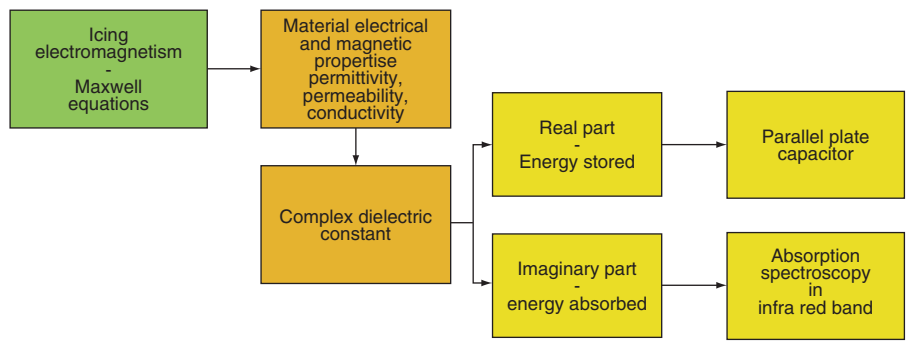

(a) Dielectric approach

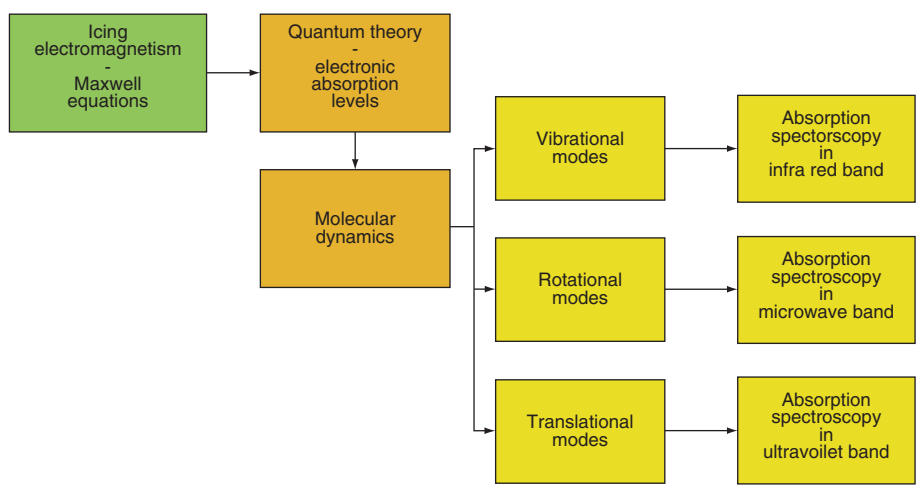

(b) Quantum approach

Figure 2 Paper Orientation - A Summary.

1.3. USING ELECTROMAGNETISM PRINCIPLES FOR ICING SENSOR

The nuclei of molecules, far from occupying fixed positions with respect to each other, are in a continual state of vibration, even at 0° K. *Due to the electronegativity difference of oxygen and hydrogen atoms ice molecule H_2O is a nonlinear polar molecule hence it has three* 3 *translational modes which can be detected in ultravoilet band,* 3 *vibrational modes which can be detected in infra red band and* 3 *rotational modes which can be detected in microwave band. The mere existence of a permanent dipole moment in water provides structural information about the molecule: it demonstrates the absence of a molecular center of symmetry and strong dielectric variations. Hence nature itself paved the way to use Electromagnetism principles for icing sensor.*

2. MOLECULAR ELECTROMAGNETISM

2.1. DYNAMIC EQUATION OF MOTION OF ELECTRON MOTION

As mentioned in [19] that the electron orbiting a nucleus is like a harmonic oscillation with a natural frequency ω_o. The dynamic equation can be defined as,

$$m\frac{d^2\Delta x}{dt^2} = -\gamma\Delta x - ZqF_{loc} \tag{1}$$

where Δx is the electrons displacement, m is the electron mass, q is the electronic charge, Z is the number electrons involved, F_{loc} is the local field acting on the atoms, and γ is the force constant. Also the natural oscillation frequency is given as $\omega_o = \sqrt{\frac{\gamma}{m}}$.

Also oscillating electron is equaivalent to an electric dipole and would radiate energy according to electromagnetic theory of radiation. This energy can be taken as a damping mechanism and $\beta\frac{dx}{dt}$ is a retarding force, hence our dynamic equation is,

$$m\frac{d^2\Delta x}{dt^2} + m\omega_o^2\Delta x = -\beta\frac{dx}{dt} - ZqF_{loc} \tag{2}$$

Also from Bohr's Model, we have the potential of electron given as,

$$E = \hbar\omega_o = \frac{mq^4}{(4\pi\varepsilon_o)^2\hbar^2} \tag{3}$$

where $\hbar = \frac{2}{\pi}$ and h is plank's constant. Also when $Z = 1$ we have electronic polarization, $\alpha_e = 4\pi\varepsilon_o R^3$ where R is radius of the ground state orbit of Bohr's atom.

Similarly electronic susceptibility and dielectric constant is given as,

$$\begin{aligned} \chi_e &= \frac{N\alpha_e}{\varepsilon_o} = \frac{N}{\varepsilon_o}\left[\frac{(Zq)^2}{m\omega_o^2}\right] \\ \varepsilon_r &= 1 + \chi_e = 1 + \frac{N}{\varepsilon_o}\left[\frac{(Zq)^2}{m\omega_o^2}\right] \end{aligned} \tag{4}$$

2.2. COMPLEX DIELECTRIC CONSTANT

The discrete nature of matter, and the behavior and interaction of those particles, can be manifested through their response to time varying electric fields with wavelengths comparable the distances between the particles.

- Time Domain Approach: We measure the time dependent polarization immmediately after the application of a step function electric field or we meausre the decay of the polarization from an initial steady state value to zero after the sudden removal of an initial polarizing field. This decay is generally referred to as *dielectric relaxation.*
- Frequency Domain Approach: We mainly measure the dielectric constant at various frequencies of alternating excitation fields.

From the viewpoint of measuring techniques, the time domain approach is simpler than the frequency domain approach, but from the viewpoint of data analysis, the time domain approach is more complex. However both approaches should be intimately connected and should yield, in principle, the same results.

Complex Permittivity When a time varying electric field is applied across a parallel plate capacitor with the plate area of one unit and a separation of d between the plates, then the total current is given by,

$$J_T = J + \frac{dD}{dt} = J + \varepsilon^* \frac{dF}{dt} \tag{5}$$

where J is the conduction current and ε^* is defined as complex permittivity which is introduced to allow for dielectric losses due to friction accompanying polarization and orientation of electric dipoles. This may be written as,

$$\varepsilon^* = \varepsilon - j\varepsilon' = \left(\varepsilon_r - j\varepsilon_r'\right)\varepsilon_o \tag{6}$$

where ε_r is dielectric constant and ε_r' is the loss factor. Also loss tangent is defined as, $\tan\delta = \frac{\varepsilon_r}{\varepsilon_r'}$ where δ is loss angle. We can use the instantaneous energy absorbed per second per cm^3 is given by $J_T(t)F(t)$. Thus, on average, the amount of energy per cm^3 per second absorbed by the material is

$$W = \frac{\omega\varepsilon_r'\varepsilon_o F_m^2}{2} \tag{7}$$

2.2.1. DIELECTRIC RELAXATION - TIME DOMAIN APPROACH

This is a time domain approach which provides conspicuous information abouth the nonlinearity of the dielectric behavior simply by varying the amplitude of the applied step function held. Experimental arrangement for the measurements of the time domain response (i.e. the transient charging or discharging current, resulting from the application or the removal of a step DC voltage) is given in Fig. 3.

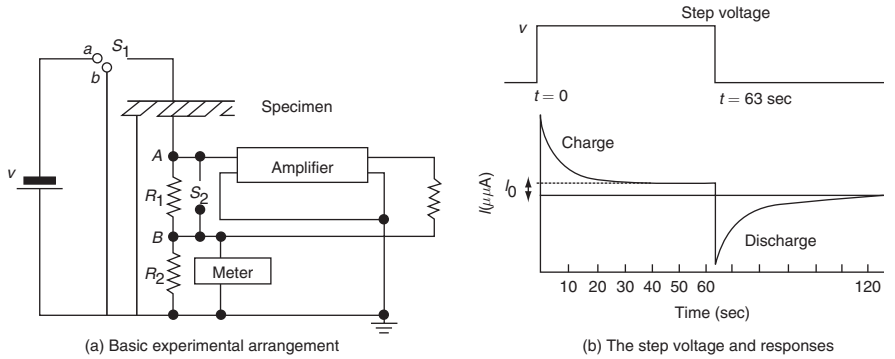

Figure 3 Setup for the measurements of the charging and the discharging current from the application and removal of a step voltage [28].

In this circuit switch S_1 has 2 positions: one for turning on the step DC voltage to start the flow of charging current, the other for short circuiting the specimen to allow the discharging current to flow after the specimen has been fully charged to a steady state level. The switch S_2 is used to shord circuit R_1 to provide a path for surge currents for a very short period of time to protect the circuit; it also gives a chance to adjust the amplifier to a null position before recording the transient current. It is important to make the time constant of the amplifier which depends on the stray capacitance in shunt with R_1, much smaller than the time during which the transient current is flowing. The specimen has the guard and the guarded electrodes, the outer guard electrode being connected to ground to eliminate surface leakage currents from the specimen. The charging or discharging current is measured as a voltage appearing across R_1 by means of a DC amplifier. The voltage drop from point A to ground is made zero by a negative feedback in the amplifier circuit, which produces a voltage across R_2 equal and opposite to that across R_1 thus making the applied step voltage across the specimen only. The step voltage and the charging and discharging current as a function of time are also shown in Fig. 3(b) in which I_o is the steady DC compoent of the charging current and the width of the step voltage is 63 seconds.

2.2.2. FREQUENCY DOMAIN APPROACH

No material is free of dielectric losses and therefore no material is free of absorption and dispersion which reflects that no material is frequency independent ε_r and $\varepsilon_r^{'}$. Now using Debye Equations for a varying electric field $F_m e^{j\omega t}$ we have the relationships as,

$$\varepsilon_r = \varepsilon_{r\infty} + \frac{\varepsilon_{rs} + \varepsilon_{r\infty}}{1 + \omega^2 \tau_0^2} \tag{8}$$

$$\varepsilon_r^{'} = \frac{\left(\varepsilon_{rs} - \varepsilon_{r\infty}\right)\omega\tau_0}{1 + \omega^2 \tau_0^2} \tag{9}$$

$$\tan\delta = \frac{\varepsilon_r^{'}}{\varepsilon_r} = \frac{\left(\varepsilon_{rs} - \varepsilon_{r\infty}\right)\omega\tau_0}{\varepsilon_{rs} + \varepsilon_{r\infty}\omega^2\tau_0^2} \tag{10}$$

Eq(s). 8, 9, 10 equations can also be written as,

$$\frac{\varepsilon_r - \varepsilon_{r\infty}}{\varepsilon_{rs} - \varepsilon_{r\infty}} = \frac{1}{1+\omega^2\tau_0^2} \tag{11}$$

$$\frac{\varepsilon_r^{'}}{\varepsilon_{rs} - \varepsilon_{r\infty}} = \frac{\omega\tau_0}{1+\omega^2\tau_0^2} \tag{12}$$

Now the Eqn(s). 11, 12 are the parametric equations of a circle in the $\varepsilon_r - \varepsilon_r^{'}$ plane. By eliminating $\omega\tau_0$ from Eq. 11 and 12 we obtain,

$$\left(\varepsilon_r - \frac{\varepsilon_{rs} + \varepsilon_{r\infty}}{2}\right)^2 + \varepsilon_r^{'2} = \left(\frac{\varepsilon_{rs} - \varepsilon_{r\infty}}{2}\right)^2 \tag{13}$$

Only the semicircle of Eqn(s). 13 over which $\varepsilon_r^{'}$ is positive has physical significance. In this Argand Diagram shown in Fig. 4(b) frequency not explicitely shown. The variation of ε_r and $\varepsilon_r^{'}$ due to the variation of ω is shown in Fig. 4(a) which illustrates schematically the typical dispersion behavior for polarization in the relaxation regime. Also the Eq(s). 8, 9, 10 are based on the following assumptions for simplicity: the local field is the same as the applied field F; the conductivity of the materials is negligible; all dipoles have only one identical relaxation time τ_o.

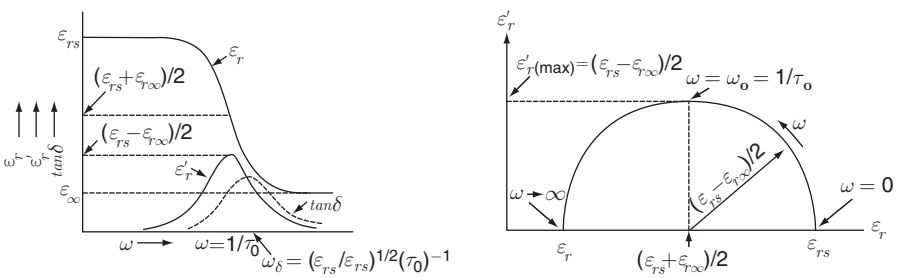

(a) $\varepsilon_r, \varepsilon_r^{'}$ and $tan\delta$ as functions of ω

(b) Argand diagram of $\varepsilon_r - \varepsilon_r^{'}$ relations for cases with one one relaxation time τ_o

Figure 4 Frequency domain approach for measurement of dielectric constants [19].

3. ICE ELECTROMAGNETISM

Molecular dimensions The dimensions of the water molecule depend on the quantum state of the molecule. For each vibrational state, the molecular dimensions may be described by three 'effective moments of inertia'. In [8] gave the following expressions for the effective moments of intertia of the water molecule as functions of its vibrational states.

$$\begin{aligned} I^{x^*} \times 10^{40}\, g\, cm^2 &= 2.9436 + 0.0611\left(v_1 + \frac{1}{2}\right) + 0.0385\left(v_2 + \frac{1}{2}\right) + 0.0441\left(v_3 + \frac{1}{2}\right) \\ I^{z^*} \times 10^{40}\, g\, cm^2 &= 1.9207 + 0.0398\left(v_1 + \frac{1}{2}\right) - 0.0249\left(v_2 + \frac{1}{2}\right) + 0.0077\left(v_3 + \frac{1}{2}\right) \\ I^{y^*} \times 10^{40}\, g\, cm^2 &= 1.0229 + 0.0213\left(v_1 + \frac{1}{2}\right) - 0.1010\left(v_2 + \frac{1}{2}\right) + 0.0486\left(v_3 + \frac{1}{2}\right) \end{aligned} \tag{14}$$

where v_1, v_2 and v_3 are the quantum numbers for the three normal modes of vibration.

Molecular vibrations The transition of a water molecule from its vibrational ground state to the excited state described by the v_2 mode is associated with the infra red absorption band centered at 1594.59 cm^{-1}. During this transition, the quantum number v_2 characterizing the v_2 mode changes from 0 to 1, while the quantum number v_1 and v_3 characterizing the v_1 and v_3 modes remain equal to zero. Similarly the transition from the ground state to the state in which only the first normal mode is excited - the state with quantum numbers v_1, $v = 0$, $v_3 = 0$ - is associated with the absorbtion band centered at 3656.65 cm^{-1}, see Fig. 2.

A simple expression involving nine empirical constants, describes the frequencies of vibrational transitions quite accurately. Let us denote $G(v_1, v_2, v_3)$ the energy above the vibrationless equilibrium state of the state with quantum numbers v_1, v_2, and v_3. Then

$$G(v_1, v_2, v_3) = \sum_{i=1}^{3} \omega_i \left(v_i + \frac{1}{2}\right) + \sum_{i=1}^{3} \sum_{k \geq i}^{3} x_{ik} \left(v_i + \frac{1}{2}\right)\left(v_k + \frac{1}{2}\right) \tag{15}$$

where the sums are over normal modes. The ω s in this equation are often called the *harmonic*

Table 2 Observed Vibrational Bands of H_2O [3].

Quantum numbers of upper state			Absorption frequencies
v_1	v_2	v_3	of band centres in cm^{-1} H_2O
0	1	0	1594.56
1	0	0	3656.65
0	0	1	3755.79
0	2	0	3151.40
0	1	1	5332.0
0	2	1	6874
1	0	1	7251.6
1	1	1	8807.05
2	0	1	10613.12
0	0	0	11032.36

Table 3 Vibrational constants of H_2O for Eqn. 15 [3].

Molecule	**H_2O**
ω_1	3832.17
ω_2	1648.47
ω_3	3942.53
x_{11}	–42.576
x_{22}	–16.813
x_{33}	–47.556
x_{12}	–15.933
x_{13}	–165.824
x_{23}	–20.332

frequencies, the xs are the *anharmonic constants* and describe the effect on the vibrational frequencies of the departure from purely harmonic from of the vibrations, see Fig. 3.

The frequency of transition between any two vibrational states can be obtained from Eqn(s) 15 and the constants from Fig(s) 3. For example, the frequency v_1 for the transition from the ground state to the state in which $v_1 = 1$, $v_2 = 0$ and $v_3 = 0$ is

$$v_1 = G(1,0,0) - G(0,0,0) = \omega_1 + 2x_{11} + \frac{1}{2}x_{12} + \frac{1}{2}x_{13} \tag{16}$$

Similarly

$$\begin{aligned} v_2 &= G(0,1,0) - G(0,0,0) = \omega_2 + 2x_{22} + \frac{1}{2}x_{12} + \frac{1}{2}x_{23} \\ v_3 &= G(0,0,1) - G(0,0,0) = \omega_3 + 2x_{33} + \frac{1}{2}x_{13} + \frac{1}{2}x_{23} \end{aligned} \tag{17}$$

Note that the anharmonic constants are negative. This means that the higher vibrational energy levels are all somewhat closer together than they would be if molecular vibrations were purely harmonic. Eqn(s) 15 also yields an expression for the zero point energy of vibration

$$\begin{aligned} \textit{Zero Point Energy} &= G(0,0,0) \\ &= \frac{1}{2}(\omega_1 + \omega_2 + \omega_3) + \frac{1}{4}(x_{11} + x_{22} + x_{33} + x_{12} + x_{13} + x_{23}) \end{aligned} \tag{18}$$

The forms of vibrations of a molecule, and hence the frequencies of the associated absorption bands, depend on the change in potential energy of the molecule during the vibration. This means that the spectrum of a molecule contains a great deal of information about the potential energy function that desribes its vibrations.

Electrical properties The mere existence of a permanent dipole moment in water provides structural information about the molecule: it demonstrates the absence of a molecular center of symmetry. Debye method is used, in which the dielectric constant of the vapour is measured as a function of temperature.

The change of the dipole moment of a molecule during the course of a vibration is related to the intensity of the corresponding absorption band. More precisely the square of the change of dipole moment with change in a normal coordinate is proportional to the integrated intensity of the band.

3.1. DIELECTRIC CONSTANT OF ICE

The static dielectric constants, ε_0 of both poly crystalline and single crystals of ice have been carefully determined [1, 18]. Fig(s) 5a shows that ε_0 increases with decreasing temperature and that ε_0 parallel to the c-axis is slightly larger than ε_0 perpendicular to the c-axis. The dielectric constant of polycrystalline ice is higher at 0°C than that of water, even though the decrease in the volumen of water on melting would be expected to cause a change in the opposite direction. The application of pressure to ice I increases ε_0, as shown in 6a.

The dielectric properties of the high pressure polymorphs were investigated by [29, 30]. [29] measured values of ε_0 for ices II, III, V and VI over a range of temperatures and pressures; their results for a constant temperature of – 30°C are shown in Fig(s). 6b. They found that with the exception of ice II, each of these polymorphs has a larger value of ε_0 than all polymorphs stable at lower pressures. Ice II has a low value of ε_0 (4.2), which is independent of temperatures and pressure. [30] found that ε_0 for ice VII at 22°C and 21 kbars is roughly 150; this is somewhat smaller than ε_0 of ice VI extrapolated to the same temperature and pressure (about 185). These authors also found that ice VIII, like ice II, has a very small value of ε_0.

Frequency dependence of ε At relatively low frequencies of the applied field, over 95% of the dielectric constant ε arises from reorientation of H_2O molecules. As the frequency is

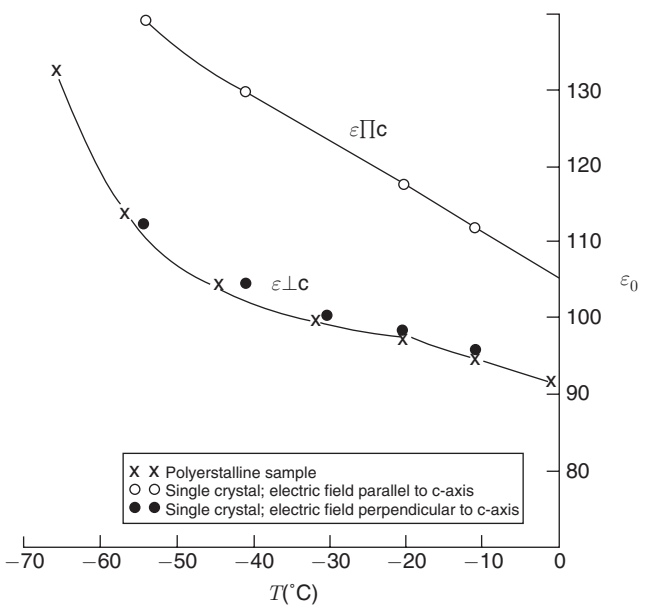

(a) The static dielectric constant of ice I, ε_0 as a function of temeperature (1,18)

Figure 5 Static dielectric coefficient of water molecule and its coordinate axes.

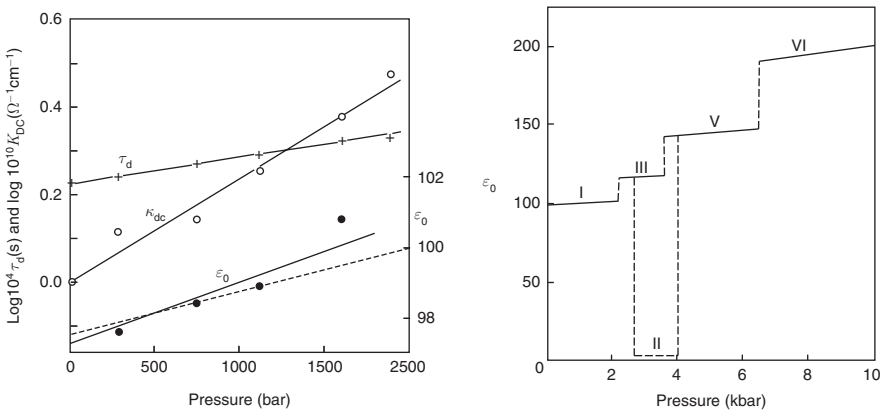

(a) Pressure dependence of the static dielectric constant (ε_0), dielectric relaxation time (τ_D) and logarithm of the direct current (κ_{DC}) of ice I at −23:40°C [5]

(b) Pressure dependence of the static dielectric constant, ε_0 of ices I, II, III, V and VI at −300°C [29]

Figure 6 Dependence of $\varepsilon 0$ on pressure.

increased, molecules do not reorient fast enough to come into equilibrium with the field, and the dielectric constant falls to a much smaller value, ε_∞. This phenemenon is called *dielectric dispersion* and can be described for many substances by a simple equation by Smyth 1955:

$$\varepsilon = \varepsilon_\infty + \frac{\varepsilon_0 - \varepsilon_\infty}{1 + (\omega \tau_D)^2} \tag{19}$$

where τ_D is the *dielectric relaxation time*, and ω is 2π times the frequency of the applied field in cycles per second. The quantity τ_D reflects the time for decay of macroscopic polarization of the substance when the external field is removed. It is somewhat larger than the molecular rotational correleation time, τ_{rd}, which is the average interval between reorientations of a given molecule. The value of τ_D for ice I at 0°C is about 2×10^{-5}s, so that an average H_2O molecule experiences roughly 10^5 reorientations every second.

$$\tau_D = \left(\frac{3\varepsilon_0}{2\varepsilon_0 + \varepsilon_\infty} \right) \tau_{rd} \tag{20}$$

It is important to realize that the reorientation of molecules is caused by thermal agitaiton, and takes place whether or not an alternating electric field is applied to the system. The applied electric field, in fact, biases reorientation of molecules to only a very small extent. This was noted for the case of ice by Debye 1929, who based his argument on the fundamental equation of electric polarization

$$\varepsilon_0 - 1 = \frac{4\pi \mathbf{P}}{\mathbf{E}} \tag{21}$$

Here **P** is the electric dipole moment per unit volume induced by the applied field **E**. Debye used this equation to that if ice at 0°C is placed in an electric field of $1\,\mathrm{Vcm}^{-1}$, the net degree of orientation of the water dipoles in equivalent to the rotation by 180° of only one molecule in 10^6. The high frequency dielectric constant, ε_∞, is temperature independent.

Frequency dependence of ε of ice polymorphs The dielectric relaxation times of the ice polymorphs in which the molecules are free to rotate may be expressed in the form,

$$\tau_D = Ae^{\left\{\frac{E_A}{RT}+\frac{\Delta V(P-P_0)}{RT}\right\}} \tag{22}$$

where P_0 is a reference pressure and A, E_A and ΔV are the experimentally determined parameters that are listed in [10]. The quantities E_A and ΔV are called the energy and volume of activation for dielectric relaxation. In [29] it is found that the relaxation of the high pressure ices cannot be precisely described by a single relaxation time for each ice. The parameter α indicates the deviation of the frequency dependence of each ice form that given by Eqn. 19. This parameter can assume values from 0 (for a single τ_D) to 1; the largest α among the ices is 0.05 for ice VI.

4. CONCLUSION

During this review study it is found that due to nonlinear polar characteristics of water molecule there is lot of potential avaiable to predict the different forms of water particularly in the domain Temp < 0. Ice being the most diversified phase of water has a good dielectric constant which can be measured effectively using different techniques as like time domain dielectric measurement techniques or frequency domain dielectric measurement techniques. Also due to the diversified characteristics of ice e.g rime and glaze ice we can use different spectroscopy techniques in the infra red, microwave or ultravoilet frequency ranges to measure the desired parameters as like ice type, icing rate and ice thickness together.

REFERENCES

[1] Auty R. P. and Cole R. H., *J. chem Phys.* 20, 1309, 1952.

[2] Benedict W. S., Gailar N., Plyer E.K., *Journal of Chemical Physics*, 21, 1301, 1953.

[3] Benedict W. S., Claassen I-I. I-I. and Shaw J. I-I, Journal of Chemical Physics, 24, pp 1139, 1956.

[4] Bertie J. E. and Whalley E., *J. chem. Phys.* 40, 1637, 1964.

[5] Chan R. K., Davidson D. W. and Whalley E., *J. chem. Phys.* 43, 2376, 1965.

[6] Cottrell T.L., *The strengths of chemical bonds*, Butterworths, London, 1958.

[7] Craig D. F. and Craig D. B., *An investigation of icing events on haeckel hill*, Proceedings of Boreas III Conference, Finland, 1995.

[8] Darling B. T. and Dennison D. M., Phys Rev. 57, 128, 1940.

[9] Dennison D. M., *Rev. mod. Phys*, 12, 175, 1940.

[10] Eisenberg D. and Kauzmann W. *The Structure and Properties of Water*, Oxford University Press, 1969.

[11] Fikke S., et. al., *Cost 727 - Atmospheric icing on structures; measurement and data collection on icing*, ISSN 1422-1381, MeteoSwiss, 2007.

[12] Foder H. F., *ISO 12494 - Atmospheric icing on structures and how to use it*., Proc. of the llth International Offshore and Polar Engineering Conference, ISBN 1-880653-51-6, June 2001.
[13] Haas C. and Hornig D. F., *J. chem Phys*. 32, 1763, 1960.
[14] Herzberg G., *Molecular spectra and molecular structure*, 2nd Edn., Van Nostrand, New York, 1950.
[15] Homola M. C., Nicklasson P. J. and Sundsbo P.A., *Ice sensors for wind turbines. Cold Regions Science and Technology*, 46: p. 125–131, 2006.
[16] Homola M. C., *Atmospheric icing on wind turbines; Modeling and consequences for energy production*, ISBN 978-82-471-3082-7, NTNU, 2011.
[17] Hornig D. F., White H. F. and Reding F. P., *Spectrochim. Acta*, 12, 338, 1958.
[18] Humbel F., Jona F. and Scherrer P., *Helv. phys. Acta*. 26, 17, 1953.
[19] Kao K. C., *Dielectric phenomena in solids*, Elsevier Academic Press, ISBN 0-12-396561-6, 2004.
[20] Lee H. and Seegmiller B., *Ice detector and de-icing fluid effectiveness monitoring system*, United States, 1996.
[21] Magenheim et. al., *Microwave ice detector*, US Patent 4054255, 1977.
[22] Seegmillar H. L. B., *Ice detector and deicing fluid effectiveness monitoring system*, US Patent 5523959, 1996.
[23] Seifert H., *Technical Requirements for Rotor Blades Operating in Cold Climates*, Proceedings of the BOREAS II conference, Pyhatunturi, Finland, 2003.
[24] Wagman D. D., Evans W. H., Halow I., Parkes V. B., Bailey S. M. and Schv R. H., Miao J., *National Bureau of Standards Technical Note*, 270-1, 1965.
[25] Wallace R. W. et. al., *Ice Thickness Detector*, US Patent 6384611 Bl, 2002.
[26] Watkins et. al., *Ice detector*, US Patent 4604612, 1986.
[27] Weinstein et. al., *Ice sensor*, US Patent 4766369, 1988.
[28] Williams G., *Polymers*, 4, 27, 1963.
[29] Wilson G. J., Chan R. K., Davidson D. W. and Whalley E., *J. chem. Phys*. 43, 2384, 1965.
[30] Whalley E., Davidson D. W. and Heath J. B. R., *J. chem. Phys*. 45, 3976, 1966.